SPLART: Articulation Estimation and Part-Level Reconstruction with 3D Gaussian Splatting

Supplementary Material

6. 3D Gaussian Splatting

3D Gaussian Splatting [26] (3DGS) is a method for reconstructing 3D scenes from posed images by representing the scene using Gaussian distributions in a continuous 3D space. Given a Gaussian blob parameterized by (μ, R, S, σ), where $\mu \in \mathbb{R}^3$ denotes the position of the center (mean) of the Gaussian, $R \in \mathbb{R}^{3\times3}$ is a rotation matrix that denotes its orientation, $S \in \mathbb{R}^{3\times3}$ is the scale matrix (the scale matrix and rotation matrix determine the covariance matrix of the Gaussian), and $\sigma \in \mathbb{R}^+$ denotes its opacity. By design, the influence of a Gaussian on a point $\mathbf{x}$ is given by

$$\begin{aligned} &g(\mathbf{x}|\mu, R, S, \sigma) \\ &= \sigma \exp\left(-\frac{1}{2}(\mathbf{x}-\mu)^T \left(RSS^TR^T\right)^{-1}(\mathbf{x}-\mu)\right). \end{aligned} \tag{16}$$

In practice, 3D Gaussians are first projected to 2D given the camera view, while all Gaussians intersecting with a pixel's ray are sorted by depth for alpha-compositing. Please refer to Kerbl et al. [26] and Ye et al. [63] for more technical details. Compared to Neural Radiance Fields [38] (NeRFs), which represent a scene with radiance and density fields in the form of neural networks, 3DGS offers a much faster rendering speed (more than $100\times$ speed-up) thanks to the efficient rasterization of Gaussians.

7. Articulating the Gaussians

In SPLART, we articulate a Gaussian blob by (1) rotating by an angle θ around a line specified by $(\mathbf{p}, \mathbf{a})$, where $\mathbf{p}$ denotes the pivot point and $\mathbf{a}$ denotes the axis direction; and (2) translating along the same line by distance d. We then need to update the parameters of the Gaussian (μ', R', S', σ') to reflect this articulation. Further, letting $\mathbf{d}$ be the camera-to-Gaussian direction computed after the articulated motion, we want to find out the actual direction $\mathbf{d}'$ with which to query the radiance field (i.e., a spherical function represented by Spherical Harmonics).

Let $\mathbf{x}'$ be the new point that results from applying the articulated motion to $\mathbf{x}$, which follows as

$$\mathbf{x}' = R_{\mathbf{a},\theta}(\mathbf{x}-\mathbf{p}) + \mathbf{p} + d\mathbf{a}, \tag{17}$$

where $R_{\mathbf{a},\theta}$ is the matrix form of the axis-angle rotation $(\mathbf{a}, \theta)$. By definition,

$$g(\mathbf{x}' \mid \mu', R', S', \sigma') = g(\mathbf{x} \mid \mu, R, S, \sigma)\, \forall \mathbf{x}. \tag{18}$$

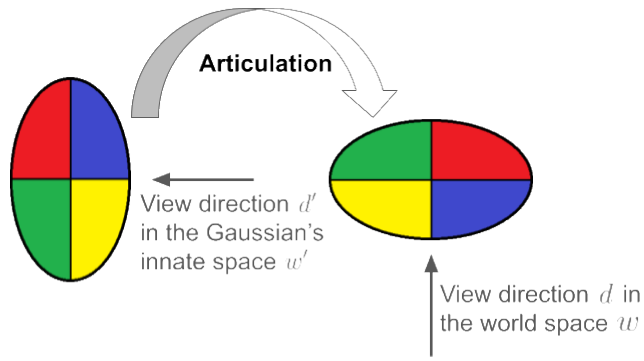

Figure 9. Since the radiance field is not modified by the articulation, we update the view direction when querying the Gaussian's radiance field in order to compensate for the articulation.

By plugging Equations 16 and 17 into Equation 18, the updated parameters follow as

$$\mu' = R_{\mathbf{a},\theta}(\mu-\mathbf{p}) + \mathbf{p} + d\mathbf{a}, \tag{19a}$$
$$R' = R_{\mathbf{a},\theta}R, \tag{19b}$$
$$S' = S, \tag{19c}$$
$$\sigma' = \sigma. \tag{19d}$$

Note that only the Gaussians are articulated, but not the radiance fields (since the coefficients of Spherical Harmonics are *not* changed). To determine the actual direction $\mathbf{d}'$ with which to query the radiance field, imagine there is a world space w' that follows the same articulated motion, meaning that w' is stationary relative to the Gaussian blob. By definition, an articulated point $\mathbf{x}'$ given by Equation 17 in the original world space w is still denoted as point $\mathbf{x}$ in w'. So

$${}^{w}T_{w'}(\mathbf{x}) = R_{\mathbf{a},\theta}(\mathbf{x}-\mathbf{p}) + \mathbf{p} + d\mathbf{a}, \tag{20}$$

where ${}^{w}T_{w'}(\cdot)$ denotes the transformation from w' to w. Now, given view direction $\mathbf{d}$ in w, the actual query direction is represented via the Gaussian's innate space, which can be computed as

$$\mathbf{d}' = {}^{w'}T_{w}(\mathbf{d}) \tag{21a}$$
$$= {R_{\mathbf{a},\theta}}^{-1}\mathbf{d}. \tag{21b}$$

See Figure 9 for an illustration.

8. Implementation

SPLART leverages *nerfstudio* [53] and *gsplat* [63], widely used open-source libraries for neural rendering and Gaussian splatting, respectively. We apply consistent hyper-parameters across all experiments, spanning synthetic and real-world datasets. Optimization stages vary in termination criteria: those driven by geometric consistency—Stages 2(a), 3(a), and 3(c)—halt upon convergence, assessed by the loss function's rate of change, whereas those guided by photometric loss—Stages 1, 2(b), and 3(b)—stop after fixed iterations of 10 000, 5000, and 10 000, respectively. By contrast, *splatfacto* (*nerfstudio*'s default 3DGS implementation) uses 30 000 iterations. In Stage 3(a), we set $K^{\mathrm{m}} = K^{\mathrm{cm}} = 3$ by default, with each optimization trial lasting 10 seconds to 1 minute on an RTX 2080 Ti. Consequently, SPLART 's total training time, approximately 20–30 minutes, is roughly twice that of *splatfacto*. For comparison, PARIS [30] requires 15–20 minutes, while DTA [60], including its LoFTR pixel-matching step, takes 35–45 minutes. At inference, rendering for novel view and articulation synthesis achieves 60–100 frames per second, varying with scene complexity due to the increased Gaussian count for intricate objects.

9. Robustness of Geometric Consistency

In Stage 3(a), we propose a practical strategy that involves multiple attempts using both mobile-only and cross-mobile geometric consistency for robust articulation estimation. For this approach to be effective, two prerequisites must be met: (1) a correct articulation should induce a lower loss than most, if not all, incorrect articulation estimates; and (2) the optimization should have a high likelihood of converging to the global optimum (indicated by the correctness of the articulation) for each randomized attempt, ensuring that a small number of trials is sufficient and robust. To verify that both prerequisites are satisfied, we design a dedicated experiment that involves 200 independent optimization trials: 100 using mobile-only geometric consistency and 100 using cross-mobile geometric consistency, both performed based on the model checkpoint saved at the end of Stage 2(b). A trial is deemed successful if it meets a similar but slightly relaxed criterion (since the estimated articulation is still coarse at this stage). Additionally, we rank the loss of each trial in comparison to the other trials performed under the same formulation. In light of the prerequisites above, we are interested in seeing whether successful trials tend to exhibit lower loss compared to those that are unsuccessful. Figure 10 visualizes these results as a scatter plot for a set of objects from the SPLART-PMS dataset.

10. Additional Qualitative Results

We present more qualitative results, including comparison with PARIS [30] on part-level reconstruction and articulation estimation in Figure 12, and view synthesis for interpolated articulation states in Figure 11.

11. Per-Scene Quantitative Results

We quantitatively compare SPLART with baselines [30, 60] for each scene in PARIS-PMS and SPLART-PMS. See Tab. 5, Tab. 7, and Tab. 8 for articulation estimation results on PARIS-PMS, revolute cases of SPLART-PMS, and prismatic cases of SPLART-PMS, respectively. For novel view and articulation synthesis, we further include SSIM [58] and LPIPS [66] metrics (in addition to PSNR [21]) for rendering quality evaluation, and per-category intersection-over-union ratios (in addition to mIoU): $\mathrm{IoU}_{\mathrm{s}}$ for the static part, $\mathrm{IoU}_{\mathrm{m}}$ for the mobile part, and $\mathrm{IoU}_{\mathrm{bg}}$ for the background. See Tab. 6, Tab. 9, and Tab. 10 for results on PARIS-PMS, revolute cases of SPLART-PMS, and prismatic cases of SPLART-PMS, respectively.

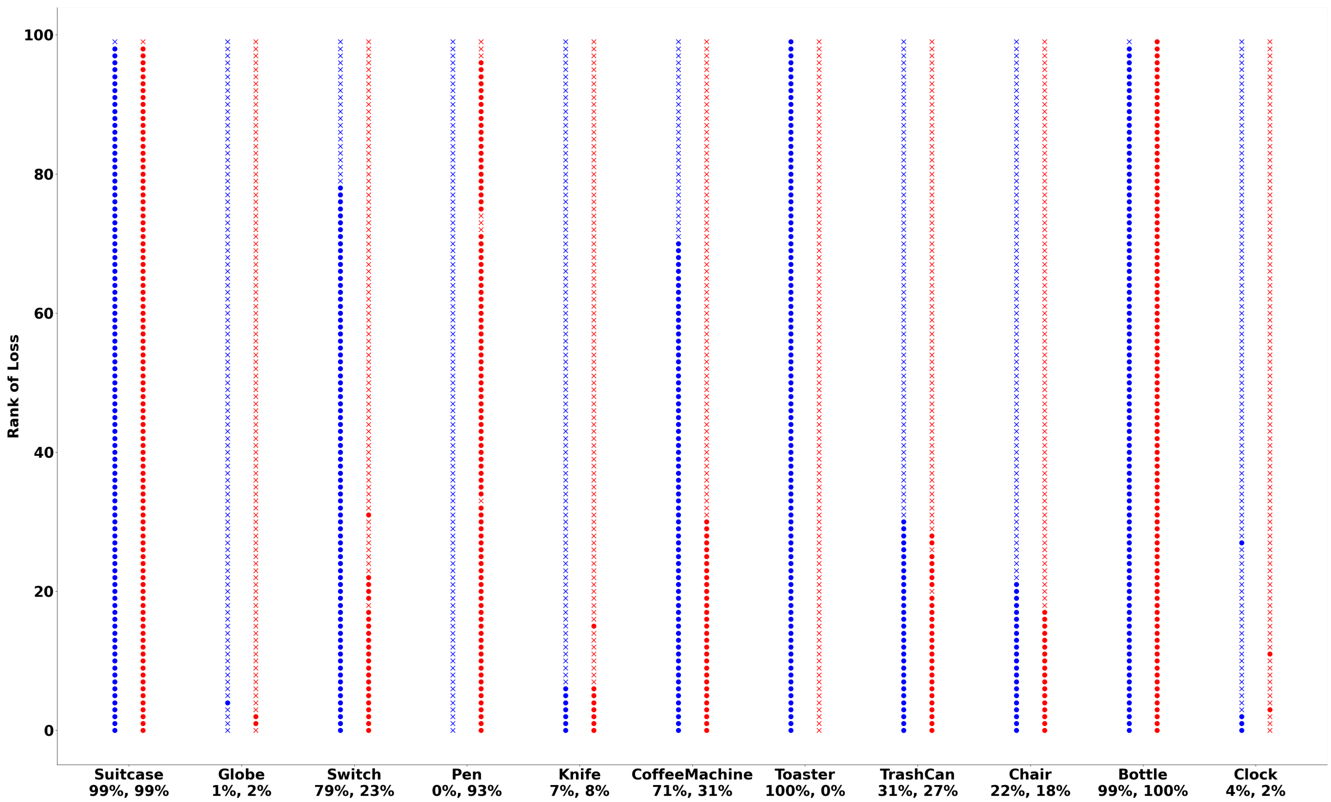

Figure 10. An analysis of the robustness of geometric consistency for articulation estimation. The horizontal axis represents different scenes, each with two columns for the two optimization formulations, where blue is used for optimization trials with mobile-only geometric consistency, and red for those with cross-mobile geometric consistency. The vertical axis represents the loss rank (lower is better). For each optimization trial, $\bullet$ denotes success, and $\times$ denotes failure. For each scene, the average success rates for both optimization formulations are shown under the scene name. Note that these success rates are the averages over the independent optimization trials and should not be confused with that of Stage 3(a) as a whole. We observe that successful trials $\bullet$ are often associated with lower losses than are failed trials $\times$, and that both optimization formulations are necessary to ensure overall robustness (e.g., *pen* requires cross-mobile geometric consistency, while *toaster* requires mobile-only geometric consistency).

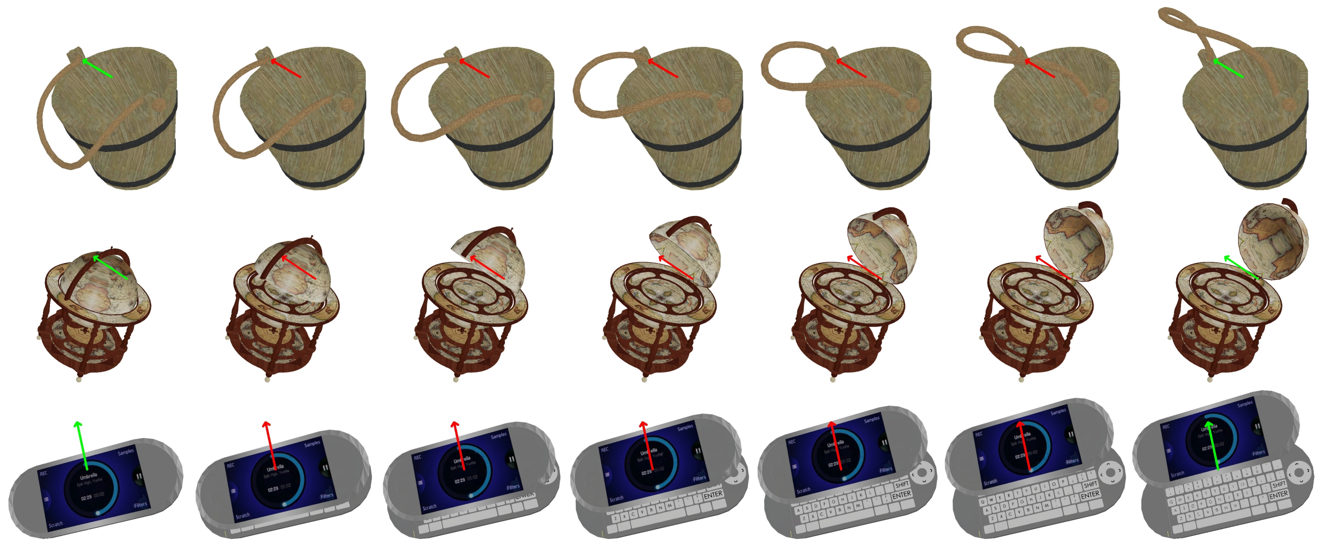

Figure 11. Additional visualizations of state interpolation for three objects along with their estimated articulation models. The left- and right-most images correspond to the ground-truth of the two end articulation states, annotated with the ground-truth articulation using green arrows. The intermediate images are rendered results obtained by interpolating the articulation state, annotated with both the ground-truth articulation (green arrows) and the estimated articulation (red arrows). Due to the high accuracy of the articulation estimation, the ground-truth green arrows are hidden by the estimated red arrows in the interpolated images.

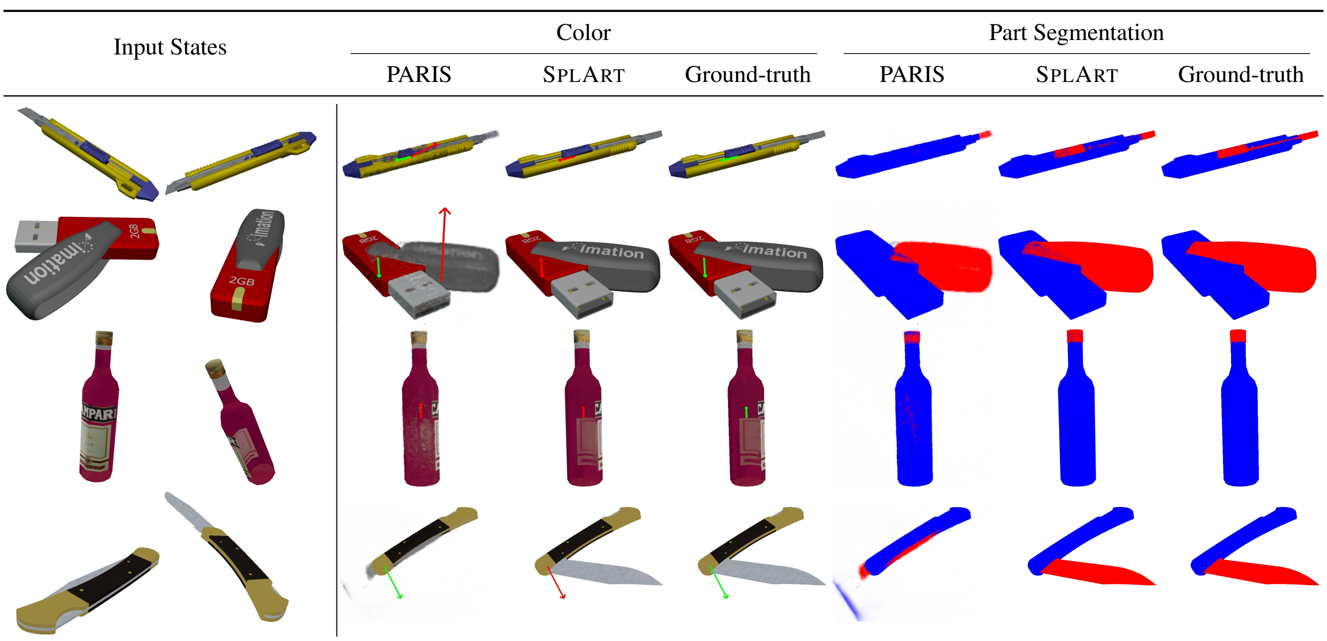

Figure 12. Additional qualitative comparisons of part-level reconstruction and articulation estimation.

Type	Scene	Method	Success Rate ↑	$\text{err}_{\mathbf{a}}$ ($\times 10^{-2}$ DEG) ↓	$\text{err}_{\mathbf{p}}$ ($\times 10^{-3}$) ↓	err_{r} ($\times 10^{-2}$ DEG) ↓	err_{t} ($\times 10^{-3}$) ↓	CD_{s} ($\times 10^{-3}$) ↓	CD_{m} ($\times 10^{-3}$) ↓	CD_{w} ($\times 10^{-3}$) ↓
Revolute	USB	PARIS	0/10	F	F	F	N/A	F	F	F
		DTA†	10/10	9.30 ± 1.29	0.39 ± 0.31	14.81 ± 3.49	N/A	2.62 ± 0.06	1.48 ± 0.03	1.36 ± 0.02
		SplArt	10/10	4.74 ± 0.32	0.26 ± 0.05	3.99 ± 0.26	N/A	0.89 ± 0.08	0.83 ± 0.11	0.91 ± 0.03
	foldchair	PARIS	3/10	103.68 ± 15.95	4.69 ± 4.77	195.70 ± 67.55	N/A	0.45 ± 0.09	45.34 ± 4.62	14.85 ± 1.00
		DTA†	10/10	3.34 ± 1.43	0.50 ± 0.31	9.72 ± 3.61	N/A	0.18 ± 0.00	0.14 ± 0.00	0.26 ± 0.00
		SplArt	10/10	5.47 ± 0.22	0.12 ± 0.03	8.93 ± 0.34	N/A	1.53 ± 0.68	0.33 ± 0.01	0.31 ± 0.00
	fridge	PARIS	9/10	105.51 ± 50.87	6.04 ± 4.17	121.25 ± 45.78	N/A	2.97 ± 0.19	39.11 ± 2.07	11.62 ± 0.54
		DTA†	10/10	6.67 ± 2.79	0.51 ± 0.32	12.07 ± 2.08	N/A	0.63 ± 0.01	0.29 ± 0.01	0.70 ± 0.00
		SplArt	10/10	4.14 ± 0.56	0.06 ± 0.05	5.81 ± 0.34	N/A	2.23 ± 0.05	1.21 ± 0.03	1.95 ± 0.04
	laptop	PARIS	10/10	117.26 ± 94.05	6.89 ± 5.45	99.11 ± 51.26	N/A	0.61 ± 0.33	32.43 ± 2.19	15.08 ± 1.41
		DTA†	10/10	6.65 ± 1.73	1.33 ± 0.52	11.81 ± 3.62	N/A	0.31 ± 0.00	0.14 ± 0.00	0.34 ± 0.00
		SplArt	10/10	3.20 ± 0.55	0.59 ± 0.05	4.89 ± 0.28	N/A	0.24 ± 0.00	0.34 ± 0.01	0.35 ± 0.01
	oven	PARIS	10/10	161.16 ± 112.94	3.44 ± 3.81	95.15 ± 55.90	N/A	9.89 ± 0.93	156.89 ± 43.24	10.90 ± 1.70
		DTA†	10/10	19.35 ± 4.10	1.57 ± 0.60	11.03 ± 2.19	N/A	4.61 ± 0.07	0.44 ± 0.01	4.26 ± 0.06
		SplArt	10/10	1.45 ± 0.32	0.90 ± 0.06	2.95 ± 0.27	N/A	7.10 ± 0.44	1.89 ± 3.52	6.02 ± 0.32
	scissor	PARIS	0/10	F	F	F	N/A	F	F	F
		DTA†	10/10	7.28 ± 5.05	4.84 ± 7.66	56.56 ± 95.23	N/A	1.67 ± 3.41	5.06 ± 13.99	0.42 ± 0.00
		SplArt	10/10	2.24 ± 0.17	0.24 ± 0.06	2.18 ± 0.26	N/A	0.37 ± 0.01	0.20 ± 0.01	0.25 ± 0.00
	stapler	PARIS	0/10	F	F	F	N/A	F	F	F
		DTA†	9/10	7.06 ± 5.68	1.81 ± 1.16	11.76 ± 11.74	N/A	2.93 ± 0.24	2.16 ± 0.89	2.03 ± 0.03
		SplArt	10/10	4.64 ± 0.43	0.75 ± 0.08	4.09 ± 0.28	N/A	1.17 ± 0.02	2.12 ± 0.14	1.05 ± 0.02
	washer	PARIS	0/10	F	F	F	N/A	F	F	F
		DTA†	10/10	38.95 ± 11.24	3.91 ± 2.63	27.51 ± 8.30	N/A	4.68 ± 0.11	0.40 ± 0.01	4.46 ± 0.12
		SplArt	10/10	3.76 ± 0.48	0.24 ± 0.15	5.95 ± 0.67	N/A	19.14 ± 1.27	1.59 ± 2.40	17.92 ± 1.22
	mean	PARIS	40.0%	121.90 ± 68.45	5.27 ± 4.55	127.80 ± 55.12	N/A	3.48 ± 0.39	68.44 ± 13.03	13.11 ± 1.16
		DTA†	98.8%	12.32 ± 4.16	1.86 ± 1.69	19.41 ± 16.28	N/A	2.20 ± 0.49	1.27 ± 1.87	1.73 ± 0.03
		SplArt	100.0%	3.70 ± 0.38	0.40 ± 0.07	4.85 ± 0.33	N/A	4.08 ± 0.32	1.06 ± 0.78	3.59 ± 0.21
Prismatic	blade	PARIS	0/10	F	N/A	N/A	F	F	F	F
		DTA†	10/10	25.72 ± 4.58	N/A	N/A	0.94 ± 0.14	0.49 ± 0.01	31.11 ± 0.55	0.37 ± 0.01
		SplArt	9/10	2.04 ± 0.61	N/A	N/A	0.22 ± 0.04	0.44 ± 0.01	26.60 ± 0.85	0.44 ± 0.01
	storage	PARIS	10/10	27.97 ± 13.09	N/A	N/A	4.28 ± 3.02	9.21 ± 1.94	151.78 ± 35.00	7.99 ± 0.49
		DTA†	10/10	6.79 ± 2.50	N/A	N/A	1.37 ± 0.13	4.88 ± 0.07	0.36 ± 0.00	4.07 ± 0.06
		SplArt	10/10	2.69 ± 0.26	N/A	N/A	0.45 ± 0.04	11.60 ± 0.38	6.94 ± 1.43	6.94 ± 0.27
	mean	PARIS	50.0%	27.97 ± 13.09	N/A	N/A	4.28 ± 3.02	9.21 ± 1.94	151.78 ± 35.00	7.99 ± 0.49
		DTA†	100.0%	16.26 ± 3.54	N/A	N/A	1.15 ± 0.14	2.69 ± 0.04	15.74 ± 0.28	2.22 ± 0.03
		SplArt	95.0%	2.36 ± 0.44	N/A	N/A	0.33 ± 0.04	6.02 ± 0.20	16.77 ± 1.14	3.69 ± 0.14
Overall		PARIS	42.0%	103.12 ± 57.38	5.27 ± 4.55	127.80 ± 55.12	4.28 ± 3.02	4.63 ± 0.70	85.11 ± 17.42	12.09 ± 1.03
		DTA†	99.0%	13.11 ± 4.04	1.86 ± 1.69	19.41 ± 16.28	1.15 ± 0.14	2.30 ± 0.40	4.16 ± 1.55	1.83 ± 0.03
		SplArt	99.0%	3.44 ± 0.39	0.40 ± 0.07	4.85 ± 0.33	0.33 ± 0.04	4.47 ± 0.30	4.20 ± 0.85	3.61 ± 0.19

Table 5. PARIS-PMS Articulation and Mesh Reconstruction Metrics. †DTA requires ground-truth depth.

Type	Scene	Method	PSNR ↑	SSIM ↑	LPIPS ↓	Depth MAE ↓	$\mathrm{IoU_s}$ ↑	$\mathrm{IoU_m}$ ↑	$\mathrm{IoU_{bg}}$ ↑	mIoU ↑
Revolute	USB	PARIS	F	F	F	F	F	F	F	F
		DTA†	N/A	N/A	N/A	0.022	0.864	0.892	0.996	0.917
		SplArt	45.70	0.996	0.0029	0.026	0.982	0.979	1.000	0.987
	foldchair	PARIS	33.48	0.936	0.0844	0.096	0.961	0.939	0.994	0.965
		DTA†	N/A	N/A	N/A	0.041	0.915	0.950	0.988	0.951
		SplArt	43.98	0.992	0.0119	0.037	0.981	0.980	0.999	0.987
	fridge	PARIS	32.22	0.967	0.0766	0.087	0.973	0.866	0.997	0.945
		DTA†	N/A	N/A	N/A	0.034	0.957	0.823	0.992	0.924
		SplArt	41.40	0.996	0.0101	0.045	0.986	0.917	0.999	0.967
	laptop	PARIS	31.64	0.964	0.0758	0.057	0.907	0.959	0.997	0.954
		DTA†	N/A	N/A	N/A	0.014	0.938	0.964	0.997	0.966
		SplArt	40.90	0.995	0.0096	0.026	0.931	0.975	0.999	0.968
	oven	PARIS	31.48	0.950	0.1048	0.132	0.977	0.891	0.996	0.955
		DTA†	N/A	N/A	N/A	0.038	0.981	0.946	0.993	0.973
		SplArt	41.59	0.993	0.0148	0.082	0.990	0.935	0.999	0.974
	scissor	PARIS	F	F	F	F	F	F	F	F
		DTA†	N/A	N/A	N/A	0.051	0.863	0.876	0.991	0.910
		SplArt	46.15	0.996	0.0030	0.044	0.951	0.954	0.999	0.968
	stapler	PARIS	F	F	F	F	F	F	F	F
		DTA†	N/A	N/A	N/A	0.035	0.902	0.894	0.994	0.930
		SplArt	44.81	0.994	0.0021	0.034	0.959	0.940	1.000	0.966
	washer	PARIS	F	F	F	F	F	F	F	F
		DTA†	N/A	N/A	N/A	0.016	0.991	0.888	0.998	0.959
		SplArt	43.75	0.996	0.0079	0.131	0.995	0.930	0.999	0.975
	mean	PARIS	32.21	0.954	0.0854	0.093	0.954	0.914	0.996	0.955
		DTA†	N/A	N/A	N/A	0.031	0.926	0.904	0.994	0.941
		SplArt	43.53	0.995	0.0078	0.053	0.972	0.951	0.999	0.974
Prismatic	blade	PARIS	F	F	F	F	F	F	F	F
		DTA†	N/A	N/A	N/A	0.116	0.728	0.416	0.998	0.714
		SplArt	46.15	0.998	0.0016	0.052	0.900	0.657	1.000	0.852
	storage	PARIS	33.75	0.944	0.1228	0.108	0.954	0.722	0.996	0.891
		DTA†	N/A	N/A	N/A	0.017	0.984	0.944	0.997	0.975
		SplArt	42.62	0.985	0.0481	0.037	0.951	0.850	0.999	0.933
	mean	PARIS	33.75	0.944	0.1228	0.108	0.954	0.722	0.996	0.891
		DTA†	N/A	N/A	N/A	0.066	0.856	0.680	0.997	0.844
		SplArt	44.38	0.991	0.0248	0.044	0.925	0.754	0.999	0.893
Overall		PARIS	32.52	0.952	0.0929	0.096	0.954	0.875	0.996	0.942
		DTA†	N/A	N/A	N/A	0.038	0.912	0.859	0.994	0.922
		SplArt	43.70	0.994	0.0112	0.052	0.963	0.912	0.999	0.958

Table 6. PARIS-PMS Novel View Synthesis Metrics. †DTA requires ground-truth depth.

Scene	Method	Success Rate ↑	$\text{err}_{\mathbf{a}}$ ($\times 10^{-2}$ DEG) ↓	$\text{err}_{\mathbf{p}}$ ($\times 10^{-3}$) ↓	err_{r} ($\times 10^{-2}$ DEG) ↓
2230 Chair	PARIS	1/10	44.97 ± 0.00	4.41 ± 0.00	130.66 ± 0.00
	DTA†	9/10	2.77 ± 0.79	0.18 ± 0.14	5.62 ± 2.35
	SPLART	10/10	0.33 ± 0.13	0.06 ± 0.03	0.84 ± 0.36
5477 Display	PARIS	8/10	86.76 ± 27.41	3.42 ± 3.21	133.12 ± 43.26
	DTA†	10/10	1.38 ± 0.39	0.27 ± 0.06	2.29 ± 0.55
	SPLART	10/10	1.91 ± 0.43	0.49 ± 0.25	4.10 ± 0.75
7054 Clock	PARIS	0/10	F	F	F
	DTA†	0/10	F	F	F
	SPLART	1/10	211.22 ± 0.00	1.06 ± 0.00	390.40 ± 0.00
11951 TrashCan	PARIS	0/10	F	F	F
	DTA†	0/10	F	F	F
	SPLART	10/10	1.65 ± 0.71	21.55 ± 16.33	473.55 ± 352.80
100247 Box	PARIS	0/10	F	F	F
	DTA†	0/10	F	F	F
	SPLART	8/10	0.79 ± 0.31	0.14 ± 0.10	1.99 ± 0.67
100460 Bucket	PARIS	0/10	F	F	F
	DTA†	10/10	15.09 ± 6.89	0.61 ± 0.34	24.57 ± 10.06
	SPLART	10/10	0.50 ± 0.23	0.03 ± 0.04	0.79 ± 0.36
100756 Globe	PARIS	0/10	F	F	F
	DTA†	0/10	F	F	F
	SPLART	1/10	0.72 ± 0.00	0.09 ± 0.00	3.31 ± 0.00
100794 Globe	PARIS	1/10	126.06 ± 0.00	14.17 ± 0.00	533.60 ± 0.00
	DTA†	10/10	4.59 ± 3.84	2.67 ± 1.39	108.22 ± 10.35
	SPLART	10/10	1.22 ± 0.35	0.12 ± 0.10	2.09 ± 0.50
100882 Switch	PARIS	2/10	393.07 ± 86.79	15.78 ± 4.03	342.44 ± 171.13
	DTA†	1/10	139.96 ± 0.00	2.67 ± 0.00	63.28 ± 0.00
	SPLART	10/10	19.37 ± 1.29	0.62 ± 0.23	11.20 ± 0.61
101542 Dispenser	PARIS	7/10	71.74 ± 49.72	5.44 ± 6.19	251.86 ± 267.19
	DTA†	0/10	F	F	F
	SPLART	8/10	0.75 ± 0.43	0.19 ± 0.06	11.48 ± 0.70
102400 Knife	PARIS	0/10	F	F	F
	DTA†	0/10	F	F	F
	SPLART	5/10	9.01 ± 5.46	22.59 ± 11.58	37.95 ± 15.46
103031 CoffeeMachine	PARIS	3/10	281.43 ± 90.89	12.95 ± 8.94	230.56 ± 65.56
	DTA†	0/10	F	F	F
	SPLART	10/10	1.69 ± 0.40	0.22 ± 0.14	1.98 ± 0.58
mean	PARIS	18.3%	167.34 ± 42.47	9.36 ± 3.73	270.37 ± 91.19
	DTA†	33.3%	32.76 ± 2.38	1.28 ± 0.39	40.80 ± 4.66
	SPLART	77.5%	20.76 ± 0.81	3.93 ± 2.41	78.31 ± 31.06

Table 7. SPLART-PMS Articulation Metrics on Revolute Scenes. †DTA requires ground-truth depth.

Scene	Method	Success Rate ↑	$\text{err}_{\mathbf{a}}$ ($\times 10^{-2}$ DEG) ↓	$\text{err}_{\mathbf{t}}$ ($\times 10^{-3}$) ↓
3558 Bottle	PARIS	5/10	45.83 ± 22.38	23.32 ± 12.29
	DTA†	10/10	200.52 ± 10.32	4.60 ± 0.27
	SPLART	10/10	3.82 ± 0.52	0.10 ± 0.02
12085 Dishwasher	PARIS	6/10	15.60 ± 7.00	4.67 ± 1.10
	DTA†	10/10	3.78 ± 1.96	2.46 ± 0.18
	SPLART	10/10	1.00 ± 0.14	0.24 ± 0.02
27189 Table	PARIS	3/10	23.69 ± 10.43	21.18 ± 3.03
	DTA†	10/10	15.90 ± 2.43	2.69 ± 0.45
	SPLART	10/10	0.14 ± 0.05	0.14 ± 0.01
100248 Suitcase	PARIS	0/10	F	F
	DTA†	10/10	192.55 ± 30.46	10.57 ± 1.60
	SPLART	10/10	1.22 ± 0.58	0.10 ± 0.04
101713 Pen	PARIS	0/10	F	F
	DTA†	10/10	179.16 ± 51.33	3.76 ± 1.04
	SPLART	10/10	244.39 ± 172.86	7.96 ± 2.71
102016 USB	PARIS	2/10	17.52 ± 10.01	9.53 ± 1.87
	DTA†	10/10	44.11 ± 5.59	7.34 ± 0.69
	SPLART	10/10	0.71 ± 0.33	0.49 ± 0.09
102812 Switch	PARIS	8/10	34.54 ± 18.03	9.04 ± 6.90
	DTA†	10/10	190.87 ± 8.20	38.68 ± 1.85
	SPLART	10/10	1.55 ± 0.80	0.11 ± 0.05
103042 Window	PARIS	5/10	189.87 ± 54.52	30.48 ± 9.55
	DTA†	10/10	92.93 ± 1.64	11.92 ± 0.23
	SPLART	10/10	1.55 ± 0.24	0.76 ± 0.18
103549 Toaster	PARIS	0/10	F	F
	DTA†	0/10	F	F
	SPLART	5/10	2.63 ± 0.74	0.30 ± 0.07
103941 Phone	PARIS	10/10	19.39 ± 10.07	6.51 ± 3.81
	DTA†	10/10	5.06 ± 0.42	1.28 ± 0.28
	SPLART	10/10	0.18 ± 0.09	0.20 ± 0.03
mean	PARIS	39.0%	49.49 ± 18.92	14.96 ± 5.51
	DTA†	90.0%	102.77 ± 12.48	9.25 ± 0.73
	SPLART	95.0%	25.72 ± 17.63	1.04 ± 0.32

Table 8. SPLART-PMS Articulation Metrics on Prismatic Scenes. †DTA requires ground-truth depth.

Scene	Method	PSNR ↑	SSIM ↑	LPIPS ↓	Depth MAE ↓	IoU_s ↑	IoU_m ↑	IoU_bg ↑	mIoU ↑
2230 Chair	PARIS	28.89	0.924	0.1004	0.231	0.510	0.737	0.982	0.743
	DTA†	N/A	N/A	N/A	0.098	0.764	0.857	0.980	0.867
	SPLART	32.08	0.972	0.0392	0.027	0.498	0.791	0.993	0.761
5477 Display	PARIS	34.34	0.943	0.0979	0.100	0.933	0.973	0.997	0.968
	DTA†	N/A	N/A	N/A	0.020	0.783	0.968	0.996	0.916
	SPLART	38.33	0.970	0.0379	0.020	0.804	0.971	0.999	0.924
7054 Clock	PARIS	F	F	F	F	F	F	F	F
	DTA†	F	F	F	F	F	F	F	F
	SPLART	35.54	0.985	0.0187	0.027	0.994	0.811	0.999	0.935
11951 TrashCan	PARIS	F	F	F	F	F	F	F	F
	DTA†	F	F	F	F	F	F	F	F
	SPLART	30.01	0.952	0.0560	0.083	0.920	0.735	0.980	0.878
100247 Box	PARIS	F	F	F	F	F	F	F	F
	DTA†	F	F	F	F	F	F	F	F
	SPLART	36.96	0.968	0.0409	0.030	0.989	0.987	0.999	0.992
100460 Bucket	PARIS	F	F	F	F	F	F	F	F
	DTA†	N/A	N/A	N/A	0.081	0.948	0.455	0.984	0.795
	SPLART	37.83	0.970	0.0397	0.016	0.989	0.832	0.999	0.940
100756 Globe	PARIS	F	F	F	F	F	F	F	F
	DTA†	F	F	F	F	F	F	F	F
	SPLART	36.30	0.990	0.0346	0.035	0.577	0.346	0.997	0.640
100794 Globe	PARIS	29.45	0.915	0.0965	0.115	0.974	0.937	0.996	0.969
	DTA†	N/A	N/A	N/A	0.046	0.961	0.943	0.994	0.966
	SPLART	35.47	0.980	0.0216	0.012	0.989	0.985	0.999	0.991
100882 Switch	PARIS	40.23	0.991	0.0418	0.082	0.989	0.822	0.999	0.937
	DTA†	N/A	N/A	N/A	0.020	0.976	0.676	0.998	0.883
	SPLART	44.04	0.997	0.0174	0.033	0.990	0.835	0.999	0.941
101542 Dispenser	PARIS	31.32	0.966	0.0450	0.105	0.883	0.623	0.998	0.835
	DTA†	F	F	F	F	F	F	F	F
	SPLART	36.53	0.992	0.0153	0.020	0.869	0.585	0.999	0.818
102400 Knife	PARIS	F	F	F	F	F	F	F	F
	DTA†	F	F	F	F	F	F	F	F
	SPLART	36.21	0.990	0.0215	0.041	0.986	0.874	0.997	0.952
103031 CoffeeMachine	PARIS	32.29	0.979	0.0659	0.116	0.977	0.825	0.997	0.933
	DTA†	F	F	F	F	F	F	F	F
	SPLART	37.20	0.993	0.0284	0.034	0.994	0.975	0.999	0.990
mean	PARIS	32.75	0.953	0.0746	0.125	0.878	0.820	0.995	0.897
	DTA†	N/A	N/A	N/A	0.053	0.886	0.780	0.990	0.886
	SPLART	36.38	0.980	0.0309	0.032	0.883	0.811	0.997	0.897

Table 9. SPLART-PMS Novel View and Articulation Synthesis Metrics on Revolute Scenes. †DTA requires ground-truth depth.

Scene	Method	PSNR ↑	SSIM ↑	LPIPS ↓	Depth MAE ↓	IoU_s ↑	IoU_m ↑	IoU_bg ↑	mIoU ↑
3558 Bottle	PARIS	35.75	0.981	0.0276	0.120	0.976	0.676	0.999	0.883
	DTA†	N/A	N/A	N/A	0.026	0.929	0.580	0.999	0.836
	SPLART	42.05	0.996	0.0076	0.034	0.994	0.968	1.000	0.987
12085 Dishwasher	PARIS	30.81	0.954	0.0927	0.111	0.964	0.929	0.994	0.962
	DTA†	N/A	N/A	N/A	0.113	0.873	0.773	0.982	0.876
	SPLART	35.70	0.988	0.0388	0.019	0.985	0.965	0.998	0.983
27189 Table	PARIS	29.55	0.887	0.1618	0.131	0.958	0.866	0.995	0.940
	DTA†	N/A	N/A	N/A	0.044	0.964	0.889	0.992	0.948
	SPLART	34.76	0.963	0.0560	0.035	0.979	0.949	0.998	0.975
100248 Suitcase	PARIS	F	F	F	F	F	F	F	F
	DTA†	N/A	N/A	N/A	0.025	0.986	0.574	0.998	0.853
	SPLART	39.76	0.995	0.0104	0.038	0.995	0.934	0.999	0.976
101713 Pen	PARIS	F	F	F	F	F	F	F	F
	DTA†	N/A	N/A	N/A	0.037	0.956	0.319	0.999	0.758
	SPLART	40.85	0.998	0.0135	0.028	0.981	0.789	1.000	0.923
102016 USB	PARIS	31.45	0.970	0.1005	0.191	0.731	0.583	0.994	0.769
	DTA†	N/A	N/A	N/A	0.157	0.710	0.553	0.979	0.747
	SPLART	35.08	0.987	0.0475	0.054	0.659	0.533	0.998	0.730
102812 Switch	PARIS	35.23	0.984	0.0433	0.102	0.987	0.908	0.998	0.964
	DTA†	N/A	N/A	N/A	0.024	0.970	0.616	0.996	0.861
	SPLART	38.69	0.995	0.0235	0.031	0.995	0.971	0.999	0.988
103042 Window	PARIS	29.11	0.967	0.0808	0.127	0.859	0.631	0.996	0.829
	DTA†	N/A	N/A	N/A	0.088	0.900	0.744	0.991	0.878
	SPLART	32.35	0.984	0.0499	0.039	0.868	0.695	0.999	0.854
103549 Toaster	PARIS	F	F	F	F	F	F	F	F
	DTA†	F	F	F	F	F	F	F	F
	SPLART	39.04	0.994	0.0195	0.036	0.997	0.949	0.999	0.982
103941 Phone	PARIS	34.21	0.972	0.0592	0.089	0.938	0.956	0.998	0.964
	DTA†	N/A	N/A	N/A	0.027	0.913	0.952	0.997	0.954
	SPLART	39.42	0.993	0.0219	0.020	0.971	0.980	0.999	0.984
mean	PARIS	32.30	0.959	0.0808	0.124	0.916	0.793	0.996	0.902
	DTA†	N/A	N/A	N/A	0.060	0.911	0.667	0.993	0.857
	SPLART	37.77	0.989	0.0288	0.033	0.942	0.873	0.999	0.938

Table 10. SPLART-PMS Novel View and Articulation Synthesis Metrics on Prismatic Scenes. †DTA requires ground-truth depth.